Examination of Chlorophyll Distribution in Lake Tahoe, Using the Airborne Visible/Infrared Imaging Spectrometer (AVIRIS)

Michael K. Hamilton, Curtiss O. Davis, Stuart H. Pilorz, and W. Joseph Rhea
Jet Propulsion Laboratory
California Institute of Technology
Pasadena, California

Kendall L. Carder
University of South Florida
Department of Marine Science
St. Petersburg, Florida

Abstract. An AVIRIS image was obtained for Lake Tahoe, California, on August 9, 1990, along with in situ data. Profiles of percent transmission of light, stimulated chlorophyll fluorescence, photosynthetically available radiation, and upwelling and downwelling irradiance and upwelling radiance in several spectral bands were measured in the water column, as well as the above-water spectral distribution of light. The image was atmospherically corrected using the LOWTRAN 7 atmospheric model, and the resulting image was examined for the presence of spurious periodicities. The low concentration of chlorophyll in the lake provided an increase in the upwelled radiance in the chlorophyll absorbing band, to the extent that pigment concentrations could be accurately modeled using a variant of the CZCS algorithm with the AVIRIS image. Although limnological sampling of the lake was insufficient for good statistical results, AVIRIS now appears to be useful in the mapping of surface chlorophyll in low concentrations, as are found in the oligotrophic ocean.

Introduction

Previous investigations using AVIRIS over water targets have demonstrated the presence of correlated noise in the data, and low signal to noise (S/N), which made it difficult to estimate the concentration of chlorophyll in the surface waters (Pilorz and Davis, 1990a; Melack and Pilorz, 1990). The Coastal Zone Color Scanner (CZCS) aboard the Nimbus-7 platform has been used to estimate the concentration of chlorophyll in surface waters, using ratios of reflected radiance for pairs of wavelengths that are pertinent to the absorption spectrum of the pigment (e.g., Gordon et al., 1983). Concentrations estimated in this way are obfuscated by the presence of multiple species with similar or overlapping spectra, and separation and identification of these require the finer spectral resolution of an instrument such as AVIRIS. However with limited S/N, applicability of the full spectral resolution of AVIRIS to dark targets such as bodies of water has yet to be realized. Pilorz and Davis (1990a) point out that, in order to discern a change in chlorophyll concentration of order 1 mg m^{-3}, it is necessary to resolve a signal of ~0.05 $\mu W\ cm^{-2}\ sr^{-1}\ nm^{-1}$.

AVIRIS was originally designed for land targets with 20%-50% reflectance; by comparison water targets have very low reflectances on the order of 2-5%. The first ocean data analyzed were collected from Monterey Bay in 1989, and problems such as patterned noise were discussed at length (Pilorz and Davis, 1990a,b). Subsequently, the design and engineering team has made great progress in improving the signal for ocean and freshwater studies, to the point that the signal in the visible and near IR is now over three times the original specifications.

In this study, the spectrum of upwelling radiance from Lake Tahoe, derived from the multispectral image, is compared to similar estimates made from in-water measurements, as well as theoretical values. The image is then used to estimate the concentration of chlorophyll at the surface, and the image-derived estimates are compared to bottle samples of chlorophyll and concentrations derived from in-water optical data that were collected in the lake. The average along-track and across-track power spectra are examined for the presence of significant peaks, indicating the presence of instrument-induced periodicities, and individual bands in the image are examined for the presence of large-scale banding not resolved using the spectral technique. These methods give an indication of whether the noise level of the image is still limiting the usefulness of AVIRIS for oceanographic and limnologic investigations.

Study Area

Lake Tahoe is the third largest alpine lake in the world with an average depth of 302 m and a maximum depth of 503 m. It is located at an elevation of 1906 m in the Sierra Nevada mountains on the California-Nevada border (Figure 1).

The water is extremely clear, with surface chlorophyll values <0.2 mg m^{-3}. The clarity of the water is maintained by the size of the lake itself, an effort by the local populace to divert sewage from surrounding areas, and the closed nature of the lake, in that there are no incoming tributaries.

Lake Tahoe was chosen as a study site because of its pure water and high altitude location. The low chlorophyll values are comparable to those found in the oligotrophic central gyres of the world ocean, and as such the lake represents the clear water end point in the range of oceanic and freshwater conditions. The area is easily accessible by boat and AVIRIS flyby. Its location at 1900 m in clear air (>100-km visibility) makes atmospheric correction easier and less sensitive to errors than scenes collected over marine targets. Further, the lack of a significant amount of absorption at wavelengths indicative of chlorophyll increases the signal at those wavelengths, making estimation of pigment using the wavelength-ratio method more accurate.

A dark, oligotrophic body of water such as Lake Tahoe should give a predictable multispectral image, in terms of its spatial consistency. The low level of surface chlorophyll, waste discharge from nearby communities, or significant tributary input makes the scene extremely homogeneous. Variations in this scene are unlikely to result from phytoplankton patchiness or point sources of effluent, and would most likely have been introduced by the instrument variability or noise.

Methods and Analytical Techniques

The overflight occurred at 10:30 PDT, and the plane had a heading of 110°. Solar zenith angle was 39.8°, and solar azimuth was 114.2°, so that the pilot was flying nearly directly into the sun to minimize sun glint and uneven illumination across the scene. The surface of the lake was flat and calm; wind speed was essentially zero at the time of the overflight.

In-water optical data were collected with an updated version of a Bio-Optical Profiling System (BOPS). The package is a Biospherical Instruments MER-1048 spectroradiometer which measures upwelling and downwelling spectral irradiance and upwelling spectral radiance, modified to include sensors for photosynthetically available radiation (PAR), depth, tilt, and roll. In addition, temperature, conductivity, chlorophyll fluorescence, and beam transmission were measured. The MER-1048 acquired data were averaged to four records a second. Other preprocessing included

filtering to remove obvious spikes and binning to one-meter averages. At each station, extracted chlorophyll and phaeopigments were measured on water samples immediately before or after the optical profile.

Specific absorption coefficients for particulates were obtained for surface waters and the total particulate absorption coefficient was determined, following the method of Mitchell and Kiefer (1988). Chlorophyll specific absorption coefficients were computed by dividing these measurements by the measured chlorophyll concentration. For filtered lake water absorption coefficients, the water was filtered a second time through a 0.2-μm Nucleopore filter and optical densities were measured with a Cary 2000 spectrophotometer using a 10-cm quartz cuvette. Non-pigmented particulate absorption was obtained by the hot methanol extraction method (Kishino et al., 1985), as modified by Roesler et al. (1989).

The image was corrected radiometrically, as well as for the effects of vignetting and dark current, using the calibration files provided with the data by the AVIRIS project. Atmospheric correction was performed with LOWTRAN-7 in radiance mode (e.g., van den Bosch and Alley, 1990), using a multiple-scattering midlatitude summer model with a visibility of 150 km and 1% surface albedo. The atmospheric radiance spectrum (Fig. 2a) was binned to the center wavelengths used by AVIRIS, and compared to the average radiance spectrum of the central 60x60 pixel subimage of the middle Lake Tahoe scene, which was completely over the water. The atmospheric spectrum was subtracted from the image on a band-by-band basis, yielding a corrected reflectance image to be used for the analysis. The mean uncorrected and corrected radiance spectra over the central subimage are shown in Figures 2a and 2b. Additionally, Figure 2b shows the upwelling radiance just above the surface, as calculated for each wavelength from the relationship (Gordon et al., 1988):

$$L_u^+ = \frac{E_d^+(1-\rho)(1-\bar{\rho})\ R}{Qn^2} \qquad (1)$$

where E_d^+ is the downwelling irradiance above the surface, ρ and $\bar{\rho}$ give the Fresnel reflectance for downwelling and upwelling radiation (both set equal to 0.02 for calm waters), R is the reflectance, and Q is 2π times the average cosine for upwelling radiance. Using the simplifying assumptions

$$R = \frac{E_u^-}{E_d^-}, \quad \text{and} \quad Q = \frac{E_u^-}{L_u^-} \qquad (2)$$

we arrive at the relation

$$L_u^+ = \left(\frac{0.96}{1.79}\right)\frac{E_d^+\ L_u^-}{E_d^-}. \qquad (3)$$

This agrees within a few percent of the simpler relation

$$L_u^+ = \left(\frac{0.98}{1.79}\right) L_u^- \qquad (4)$$

which was used to create the upwelling radiance depicted as the dashed line on Figure 2b. The discrete points on the figure represent, by way of another comparison, values for upwelling radiance in waters with a chlorophyll concentration of 0.15 mg m^{-3}, theoretically expected at 443, 520, and 550 nm (e.g., Gordon et al., 1988).

Selected bands of the central Lake Tahoe image, corresponding to center wavelengths 440 (band 5), 548 (band 16), and 557 (band 17) nm were examined in detail. These bands were selected because of the importance of the wavelengths to the absorption spectrum of chlorophyll, as well as to examine one band where the instrument has a higher noise level, and two adjacent bands (to look for features that persist between data channels).

For these bands, along-track and across-track power spectra were calculated as the product of the Fourier transform of each demeaned line of pixels (tapered with a Hanning windowing function) and the complex conjugate of the transform. This operation was carried out for every line of data at constant sample, or each sample on a line, resulting in the two unidirectional mean power spectra for the image.

Chlorophyll concentration was estimated for the surface waters of Lake Tahoe using the CZCS algorithm for low chlorophyll (Gordon et al., 1983), i.e.,

$$\log10[chla] = 0.053 + 1.71 \log10\left(\frac{Lw(550)}{Lw(443)}\right) \qquad (5)$$

where $L_W(550)$ and $L_W(443)$ are the values of upwelled radiance from the surface in 20 nm wide bands (full width half maximum) centered at 550 and 443 nm. The bands were approximated using the mean value of the bands bracketing each of the wavelengths, i.e., bands 5 and 6 for 440 nm, and 16 and 17 for 548 nm, which are 10 nm wide.

Results

The optical profiler data are presented in Figure 3. The temperature profile indicates a well-mixed upper 10 m, with a broad thermocline between 10 and 65 m. Chlorophyll fluorescence has a maximum at the base of the thermocline, which is indicative of a population of photosynthetically efficient phytoplankton, supported by a diffusive nutrient flux from below. Percent transmission of light is high (>90%) and is nearly uniform with depth, but with a small minimum at the base of the thermocline, caused by the phytoplankton living at that depth. PAR is attenuated with no significant deviations from the characteristic logarithmic profile that is to be expected from pure water (e.g., Smith and Baker, 1978).

Spectral absorption coefficients for pigments, particulates, and filtered water are shown in Figure 4. Near 450 nm, absorption due to gelbstoffe (dissolved organic substances) is nearly a factor of four greater than the corresponding absorption for chlorophyll and related pigments. Absorption by detritus is an order of magnitude less than absorption by pigmented particles. As expected for a clean alpine lake, these values are all very low when compared to the absorption coefficient of water.

The shape of the particulate absorption spectrum indicates the presence of chlorophyll; however the magnitude of the absorption feature near 440 nm (~0.01 m^{-1}), as well as the lack of a reduction in the upwelling radiance (L_U) at the same wavelength, implies a very low concentration. This has been verified with bottle samples. Concentration of chlorophyll in the surface waters was found to be

~0.15 mg m^{-3}, of the order expected in the oligotrophic ocean.

Figure 5 shows the standard deviation associated with the central subimage. The noise level in the blue end of the spectrum typically confounds attempts to estimate pigment concentrations. The mean signal from the image in the band closest to 440 nm is ~4 $\mu W\ cm^{-2}\ sr^{-1}\ nm^{-1}$, with a standard deviation of 0.27 giving an S/N of approximately 15:1. The mean atmospherically corrected signal has a magnitude of approximately 0.55 $\mu W\ cm^{-2}\ sr^{-1}\ nm^{-1}$, giving an S/N for the signal of ~2:1, after removing the effects of the atmosphere. To detect a change in surface chlorophyll in waters with high concentration on the order of 1 mg m^{-3}, it is necessary to resolve a signal of 0.05 $\mu W\ cm^{-2}\ sr^{-1}\ nm^{-1}$, necessitating a spatial averaging for quantitative determination of surface pigment.

The mean along-track and across-track power spectra are shown for three bands pertinent to absorption by pigments in Figure 6. Generally, band 5 shows the highest variance/cycle, as the instrument noise level is highest in the blue end of the spectrum. The along-track direction has generally featureless spectra, although some degree of spectral coherence can be seen. A high degree of power associated with the lowest frequency is probably due to the bowl shape of the vignetting effect. The lack of significant spectral peaks is to be expected from homogeneous surface concentrations of light-affecting constituents. In the across-track direction, however, there are several peaks which may be significant, and are seen to be reproducible between bands. Peaks at 0.05 and 0.065 cycles per pixel (corresponding to periodicities with spatial scales of 400 and 307 m, respectively) persist among bands 6, 16, and 17. This could be due to either low-frequency surface waves, or a vibration or electronic noise problem with the instrument. Another peak at 0.01 cpp (2000 m) is very significant and may represent a sampling problem. The fact that it gives a waveform every 100 pixels is suspicious.

Using the low-pigment variant of the CZCS algorithm (Gordon et al., 1983), an image representing surface chlorophyll concentration was constructed (Figure 7) using no spatial binning. As is to be expected, no significant pigment features are seen; the image is a low-value background, interspersed with random noise. The average estimated chlorophyll value for the center of the scene is 0.154 mg m^{-3}. This compares quite well with the value of 0.16 for the surface (5 m) sample from station 1, as well as the value of 0.15 mg m^{-3} calculated using the CZCS algorithm with the upwelling radiance values determined from the in-water measurements (Table 1).

A banding of the image is evident however, and an investigation of this phenomenon has shown it to be a ~1 DN jump, possibly due to the quantizer used to digitize the data. The mechanism for this deviation is enigmatic at this time; however the feature is not believed significant in the use of AVIRIS images for water targets.

Conclusions

Atmospherically corrected spectral radiance measured using AVIRIS agrees well with upwelling radiance derived from in-water spectral measurements and with theoretical estimates. Values of chlorophyll concentration, calculated using a variant of the CZCS algorithm with the AVIRIS image and checked with both bottle samples and in-water measurements of upwelling radiance, agree extremely well. This is in contrast to eutrophic bodies of water with high concentrations of pigment, where the signal received by the sensor is insufficient in the bands pertinent to absorption by chlorophyll to make good estimates (e.g., Melack and Pilorz, 1990). The signal-to-

noise level of AVIRIS has risen to the point where it is now useful in estimating low pigment concentrations in oligotrophic waters.

Spurious spectral peaks were found in the across-track direction of the Lake Tahoe central AVIRIS scene, and the source of these peaks warrants attention. In the image of estimated chlorophyll concentration, a banding is apparent that may be due to dark current subtraction, but is not necessarily significant in the applicability of AVIRIS images to water targets as it has a magnitude of ~1 DN.

Future modifications to the AVIRIS instrument to address the dark current and vignetting corrections over dark targets may be necessary, possibly a variable or interactive-type correction for the vignetting may be appropriate. Further, improvements in the level of signal to noise would make the data applicable without pixel binning to bodies of water with greater concentrations of absorbing pigments, such as coastal and eutrophic regions.

Acknowledgments

The authors thank the AVIRIS engineering team in general and Rob Green in particular for their continued effort to improve the performance of the instrument. We thank the AVIRIS operations team and the NASA Ames Research Center, High Altitude Branch for collecting the AVIRIS data. John Melack (U.C. Santa Barbara) organized the field work and Robert Richards (U.C. Davis) provided the ship support. Discussions with and editing by Jeannette van den Bosch were extremely helpful.

This work was carried out at the Jet Propulsion Laboratory, California Institute of Technology and at the University of South Florida, and was supported by contracts from the National Aeronautics and Space Administration to those Institutions. Reference herein to any specific commercial product, process, or service by trade name, trademark, manufacturer, or otherwise, does not constitute or imply its endorsement by the United States Government, the Jet Propulsion Laboratory, California Institute of Technology or the University of South Florida.

References

Gordon, H., D. Clark, J. Brown, O. Brown, R. Evans, and W. Broenkow, "Phytoplankton Pigment Concentrations in the Middle Atlantic Bight: Comparison of Ship Determinations and CZCS Estimates," *Applied Optics* 22 (1); 20-36, 1983.

Gordon, H., O. Brown, R. Evans, J. Brown, R. Smith, K. Baker, and D. Clark, "A Semianalytic Radiance Model of Ocean Color," *Journal of Geophysical Research* 93 (D9), 10,909-10,924, 1988.

Kishino, M., M. Takahashi, N. Okami, and S. Ichimura, "Estimation of Spectral Absorption Coefficients of Phytoplankton in the Sea," *Bull. of Mar. Sci.* 37 (2), 634-642, 1985.

Melack, J., and S. H. Pilorz, "Reflectance Spectra from Eutrophic Mono Lake, California, Measured With the Airborne Visible and Infrared Imaging Spectrometer (AVIRIS)," *Proceedings of the Second Airborne Visible / Infrared Imaging Spectrometer Workshop*, JPL Publication 90-54, Jet Propulsion Laboratory, Pasadena, California, 232-242, 1990.

Mitchell, B. G., and D. A. Kiefer, "Variability in Pigment-Specific Particulate Fluorescence and Absorption Spectra in the NE Pacific Ocean," *Deep Sea Research* 35 (5), 665-689, 1988.

Pilorz, S., and C. O. Davis, "Investigations of Ocean Reflectance With AVIRIS Data," *Proceedings of the Second Airborne Visible/Infrared Imaging Spectrometer Workshop*, JPL Publication 90-54, Jet Propulsion Laboratory, Pasadena, California, 224-231, 1990a.

Pilorz, S., and C. O. Davis, "Spectral Decomposition of Sea Surface Reflected Radiance," *Proceedings, IGARSS 1990* (1), 345-348, IEEE, 1990b.

Roesler, C. S., M. J. Perry, and K. L. Carder, "Modeling In Situ Phytoplankton Absorption From Total Absorption Spectra," *Limnol. Oceanogr.* 34 (8), 1510-1523, 1989.

Smith, R. C., C. R. Booth, and J. L. Star, "Oceanographic Bio-Optical Profiling System," *Applied Optics* 23, 2791-2797, 1984.

Smith, R. C, and K. Baker, "Optical Classification of Natural Waters," *Limnology and Oceanography* 23, 260-267, 1978.

Strickland, J. D. H., and T. R. Parsons, "A Practical Handbook of Seawater Analysis," *Fish. Res. Bd. Canada Bull.* 167, 311, 1972.

van den Bosch, J., and R. Alley, "Application of LOWTRAN 7 as an Atmospheric Correction to Airborne Visible/Infrared Imaging Spectrometer (AVIRIS) Data," *Proceedings of the Second Airborne Visible/Infrared Imaging Spectrometer Workshop*, JPL Publication 90-54, Jet Propulsion Laboratory, Pasadena, California, 78-81, 1990.

Table 1. Chlorophyll values measured at Station 1 and estimated from the optical data and the midlake AVIRIS image using the CZCS chlorophyll algorithm.

Method	depth m	Chlorophyll mg/m-3	Phaeopigments mg/m-3	Chl. + Phaeo. mg/m-3
Extracted chlorophyll	5	0.16	0.0	0.16
	50	0.37	0.0	0.37
	70	0.47	0.27	0.74
	100	0.19	0.12	0.31
Estimate from L_u data	surface	0.15		
Estimate from image	surface	0.154		

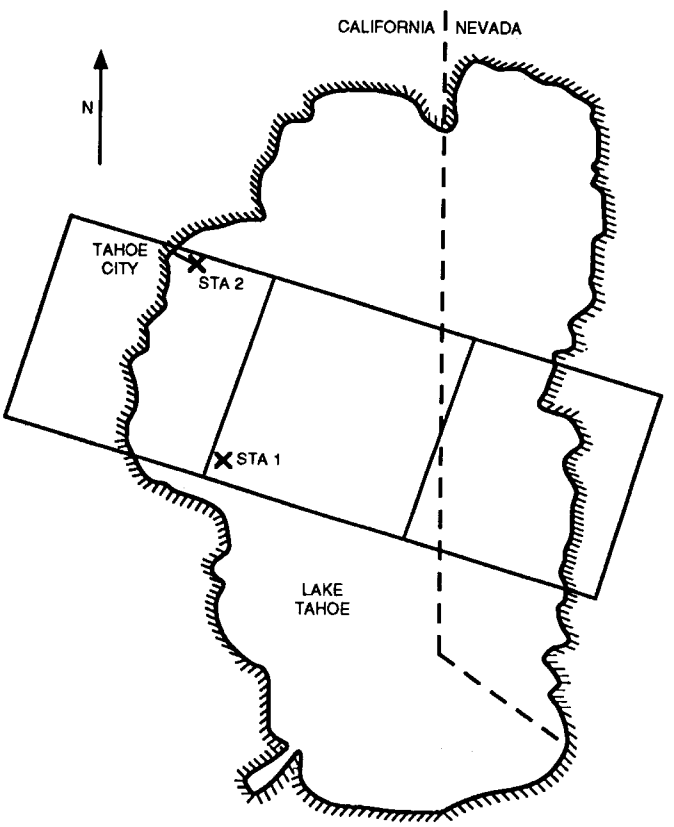

Figure 1. Map of the Lake Tahoe study site. The ER-2 flew from northwest to southeast taking three AVIRIS scenes as indicated by boxes in the figure. The in situ data presented in this paper were collected at station 1.

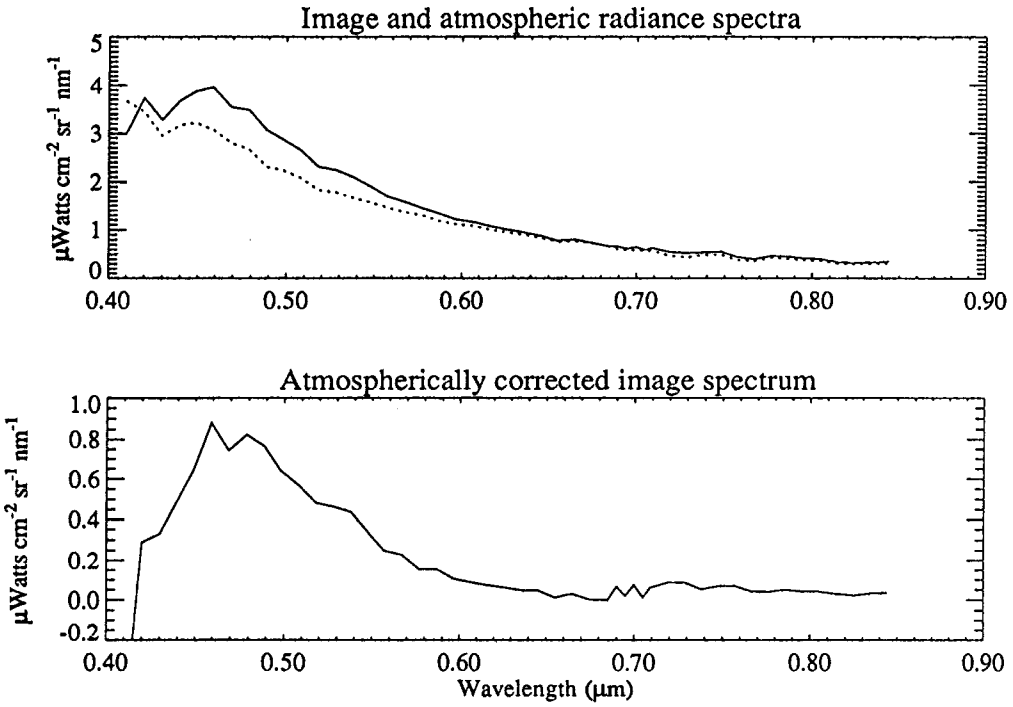

Figure 2a. Mean uncorrected image spectrum, with the modeled spectrum of atmospheric radiance, taken over the central 3600-pixel central subimage of the middle Lake Tahoe scene. Bottom panel shows difference between the two.

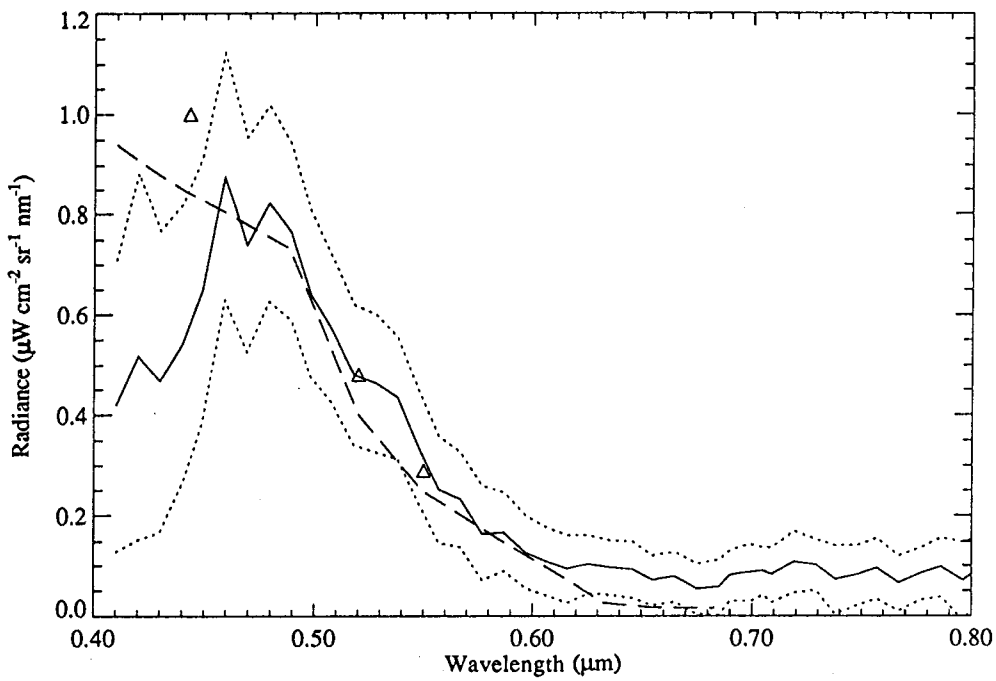

Figure 2b. Atmospherically corrected image spectrum, with a one standard deviation error envelope. The dashed line is the upwelling radiance derived from in-water measurements, and the points are the theoretical values of upwelling radiance for water with a chlorophyll concentration of 0.15 mg m^{-3}.

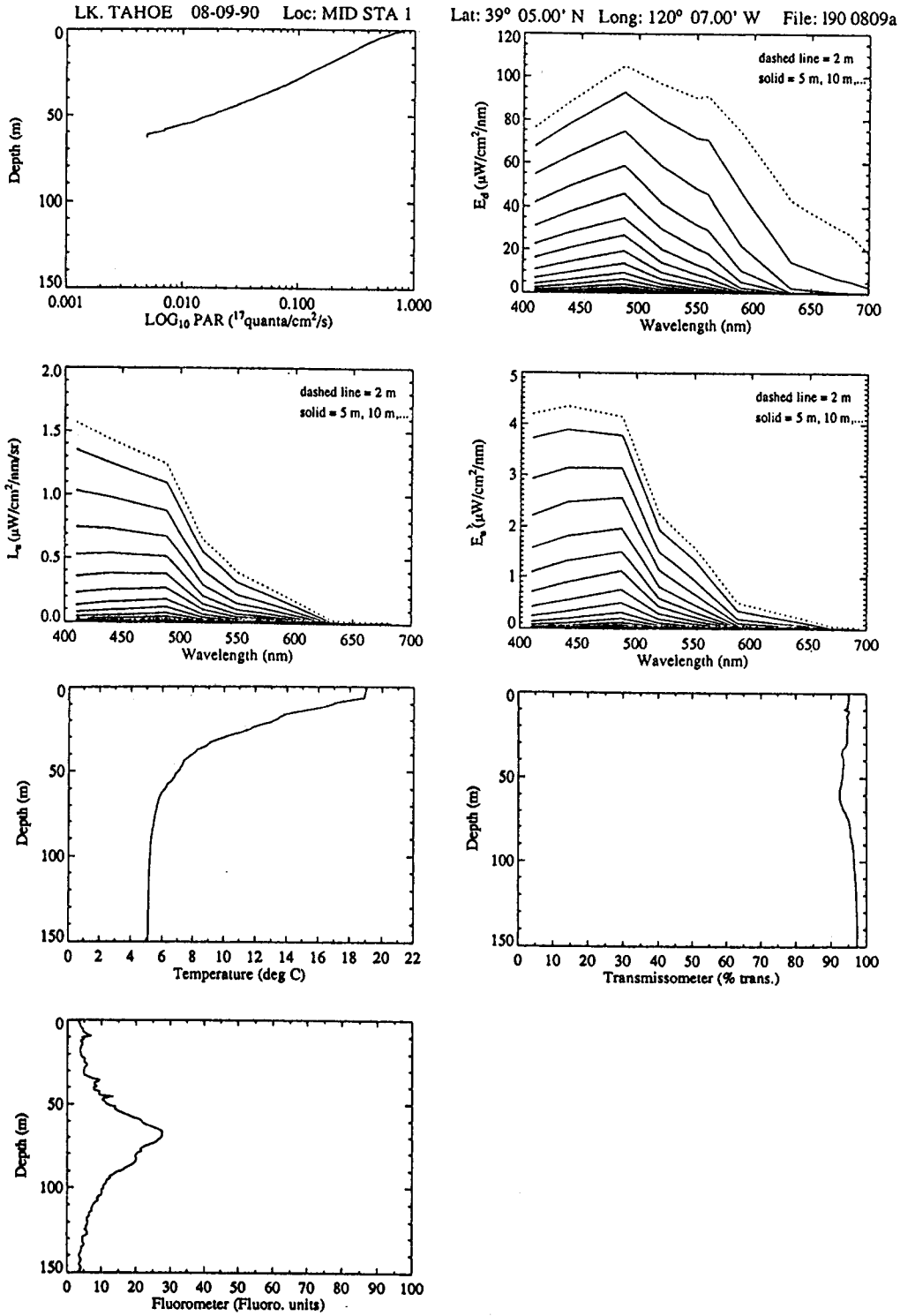

Figure 3. Data collected with the MER-1048 bio-optical profiling instrument package at station 1.

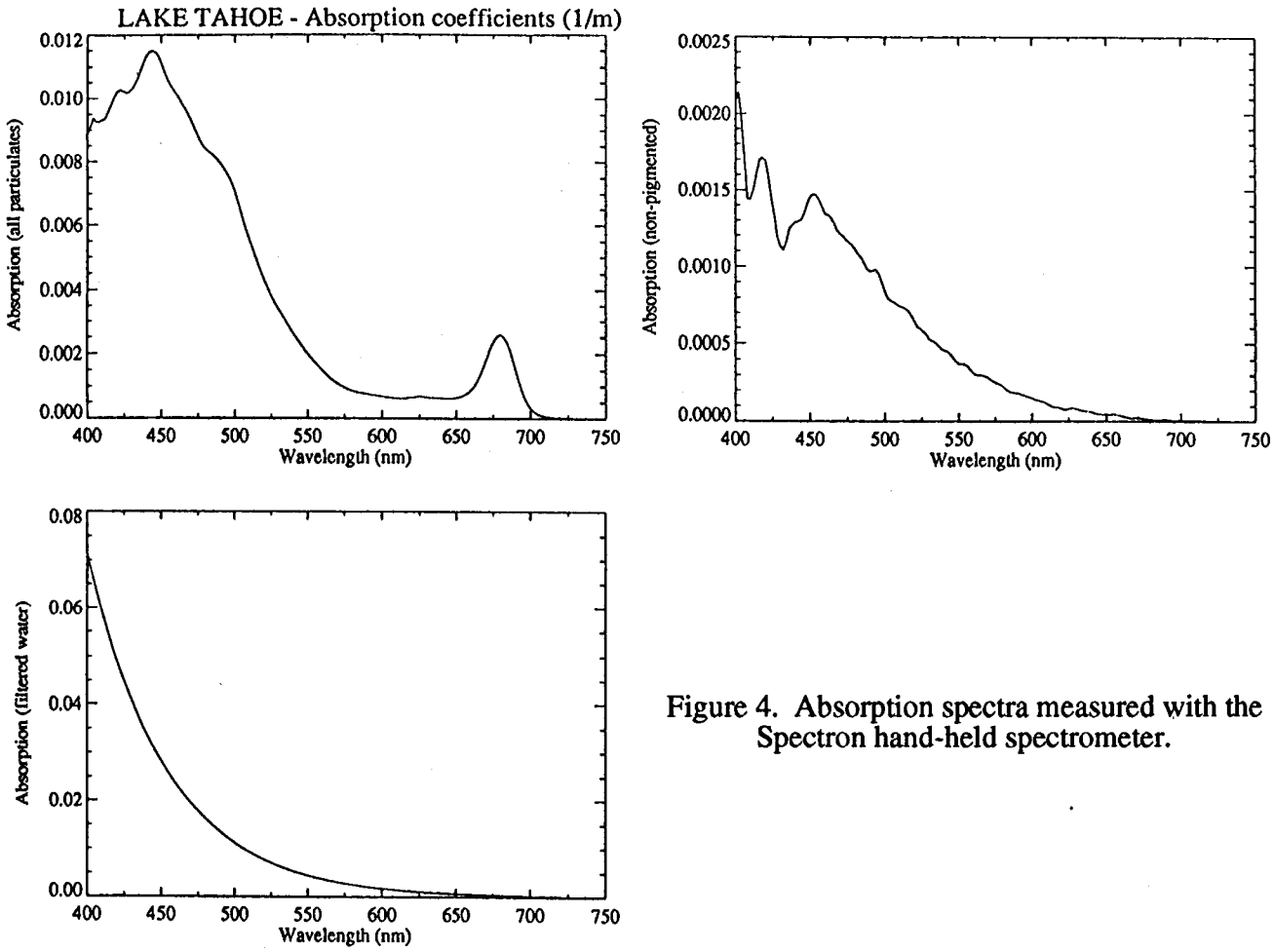

Figure 4. Absorption spectra measured with the Spectron hand-held spectrometer.

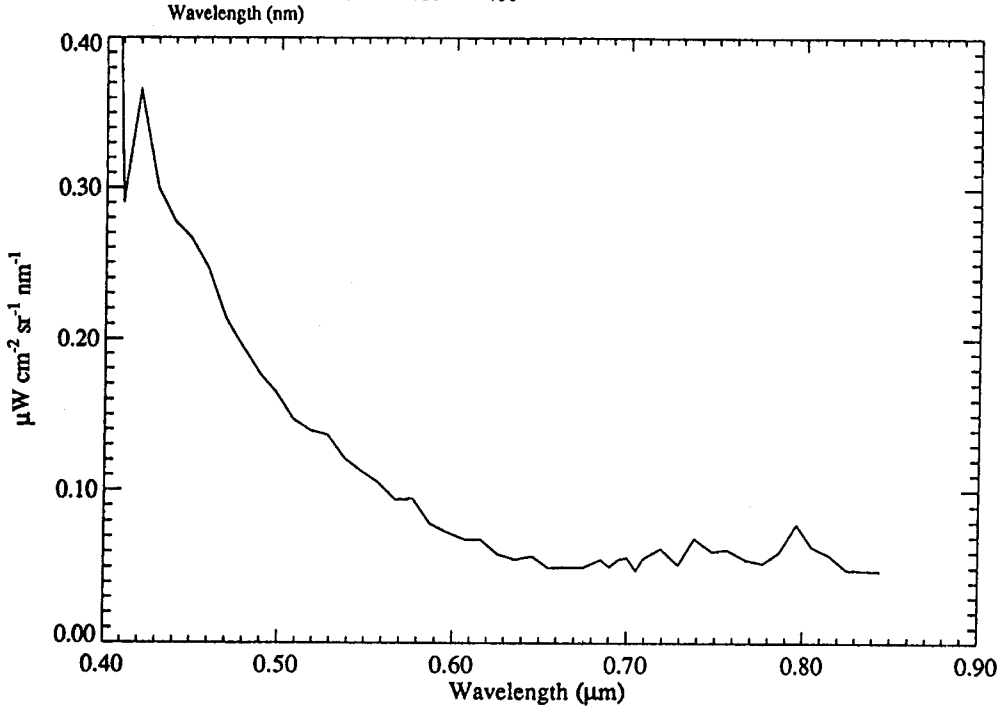

Figure 5. Spectrum of the standard deviation of the central portion of the atmospherically corrected image.

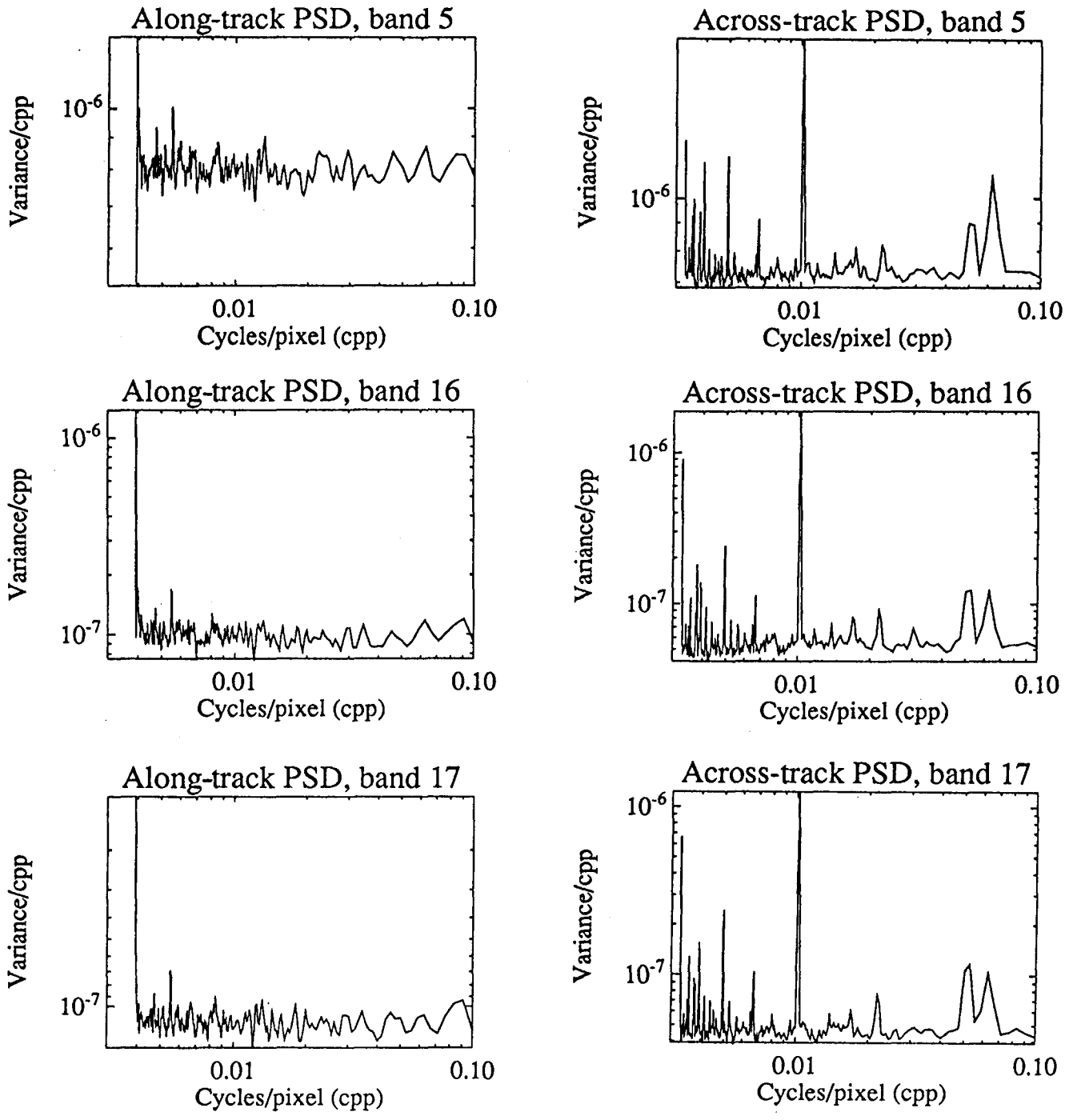

Figure 6. Along-track and across-track power spectra, for three bands from the image.

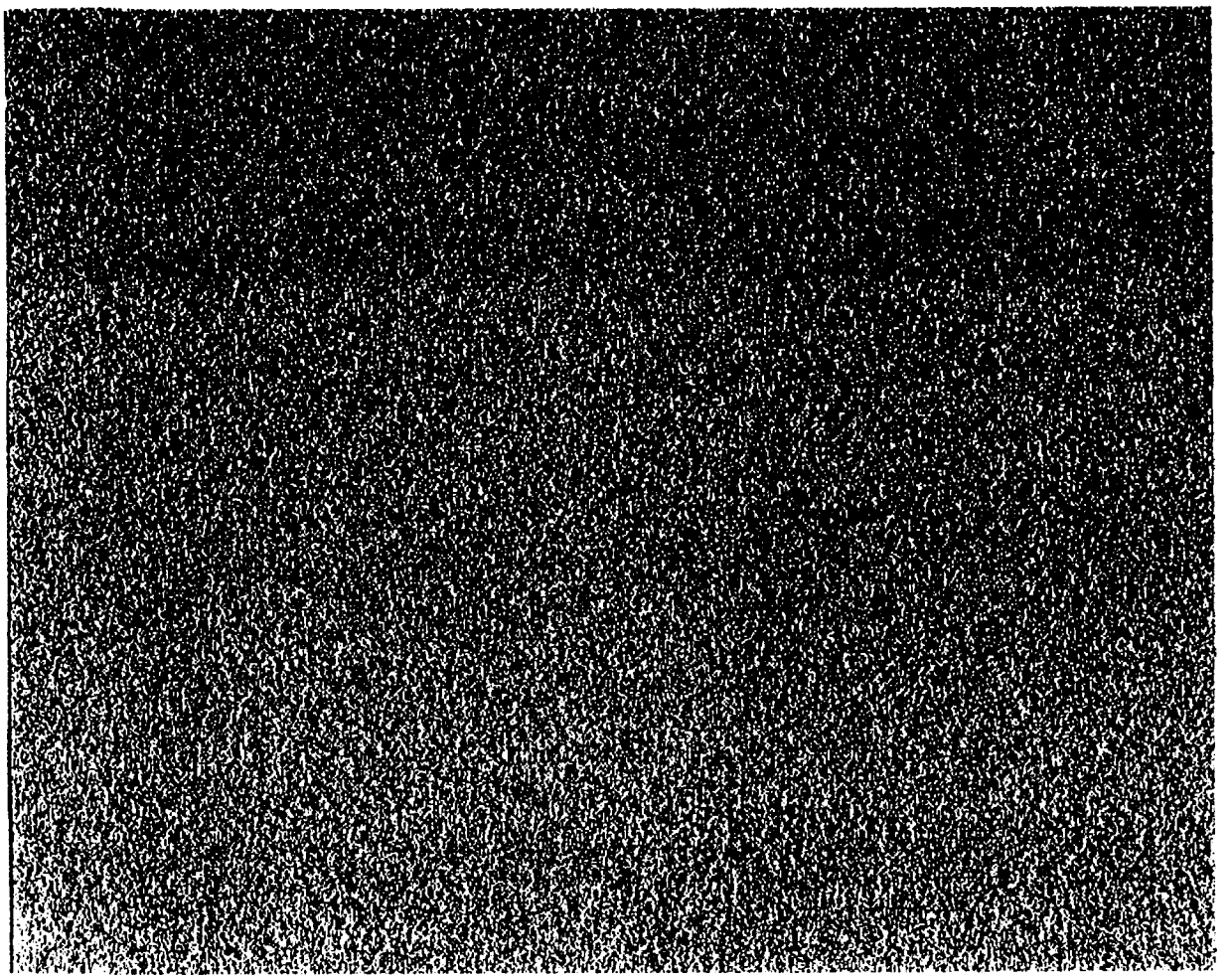

Figure 7. Image of estimated chlorophyll concentration in the surface waters. The direction of flight is toward the top of the page.